




## Article

# Design, Synthesis, Computational and Biological Evaluation of Novel Structure Fragments Based on Lithocholic Acid (LCA)

Jiangling Peng <sup>1,†</sup>, Mingjie Fan <sup>2,†</sup>, Kelly X. Huang <sup>1</sup>, Lina A. Huang <sup>1</sup>, Yangmeng Wang <sup>2</sup>, Runkai Yin <sup>1</sup>, Hanyi Zhao <sup>1</sup>, Senlin Xu <sup>2</sup>, Hongzhi Li <sup>3</sup>, Alon Agua <sup>2</sup>, Jun Xie <sup>3</sup>, David A. Horne <sup>3</sup>, Fouad Kandeel <sup>1</sup>, Wendong Huang <sup>2,\*</sup> and Junfeng Li <sup>1,\*</sup>

<sup>1</sup> Department of Translational Research and Cellular Therapeutics, Arthur Riggs Diabetes and Metabolism Research Institute, Beckman Research Institute, City of Hope National Medical Center, Duarte, CA 91010, USA

<sup>2</sup> Department of Diabetes Complications & Metabolism, Arthur Riggs Diabetes and Metabolism Research Institute, Beckman Research Institute, City of Hope National Medical Center, Duarte, CA 91010, USA

<sup>3</sup> Department of Molecular Medicine, Beckman Research Institute, City of Hope National Medical Center, Duarte, CA 91010, USA

\* Correspondence: whuang@coh.org (W.H.); juli@coh.org (J.L.); Tel.: +1-626-218-1203 (W.H.); Tel.: +1-626-218-4507 (J.L.)

† These authors contributed equally to this work.

**Abstract:** The regulation of bile acid pathways has become a particularly promising therapeutic strategy for a variety of metabolic disorders, cancers, and diseases. However, the hydrophobicity of bile acids has been an obstacle to clinical efficacy due to off-target effects from rapid drug absorption. In this report, we explored a novel strategy to design new structure fragments based on lithocholic acid (LCA) with improved hydrophilicity by introducing a polar “oxygen atom” into the side chain of LCA, then (i) either retaining the carboxylic acid group or replacing the carboxylic acid group with (ii) a diol group or (iii) a vinyl group. These novel fragments were evaluated using luciferase-based reporter assays and the MTS assay. Compared to LCA, the result revealed that the two lead compounds **1a–1b** were well tolerated in vitro, maintaining similar potency and efficacy to LCA. The MTS assay results indicated that cell viability was not affected by dose dependence (under 25  $\mu$ M). Additionally, computational model analysis demonstrated that compounds **1a–1b** formed more extensive hydrogen bond networks with Takeda G protein-coupled receptor 5 (TGR5) than LCA. This strategy displayed a potential approach to explore the development of novel endogenous bile acids fragments. Further evaluation on the biological activities of the two lead compounds is ongoing.

**Keywords:** bile acids; Takeda G protein-coupled receptor 5 (TGR5); metabolic disorders; hydrophilicity; luciferase-based reporter assay; structure–activity relationship (SAR)



**Citation:** Peng, J.; Fan, M.; Huang, K.X.; Huang, L.A.; Wang, Y.; Yin, R.; Zhao, H.; Xu, S.; Li, H.; Agua, A.; et al. Design, Synthesis, Computational and Biological Evaluation of Novel Structure Fragments Based on Lithocholic Acid (LCA). *Molecules* **2023**, *28*, 5332. <https://doi.org/10.3390/molecules28145332>

Academic Editors: Rosanna Maccari and Rosaria Ottana

Received: 7 March 2023

Revised: 30 June 2023

Accepted: 7 July 2023

Published: 11 July 2023



**Copyright:** © 2023 by the authors. Licensee MDPI, Basel, Switzerland. This article is an open access article distributed under the terms and conditions of the Creative Commons Attribution (CC BY) license (<https://creativecommons.org/licenses/by/4.0/>).

## 1. Introduction

Bile acids have long been recognized as detergents capable of solubilizing cholesterol and fatty acids to promote digestion and transport. Recent studies have revealed more expansive and profound paracrine and endocrine functions that have driven investigations on their therapeutic applications [1]. Drug development for metabolic disorders has harnessed the potential of bile acids as regulators of glucose and lipid metabolism, insulin sensitivity, and energy expenditure [2,3]. Downstream bile acid pathways have also exhibited a vast array of anti-inflammatory [4,5], cancer suppression [6,7], neuroprotection [8], viral inhibition [9], and intestinal and cardiovascular properties [10–13]. Therefore, the regulation of bile acid pathways is a promising therapeutic strategy for a host of metabolic disorders, cancers, and diseases. Due to their tremendous potential, the modulation of bile acids has arisen as an attractive approach for various therapies.

There has been corresponding growing interest in targeting the bile acid membrane receptors Takeda G protein-coupled receptor 5 (TGR5) and the farnesoid X receptor (FXR) [14]. TGR5 functions as a regulator of glucose metabolism, bile acid homeostasis, insulin secretion, and energy expenditure. As a membrane receptor, TGR5 is expressed in brown adipose tissue, skeletal muscle, the brain, the liver, the gallbladder, immune cells, and intestinal endocrine L-cells [15–19]. Meanwhile, FXR maintains energy and glucose homeostasis and liver metabolism. FXR is expressed primarily in the spleen, intestine, kidney, adrenal gland, and liver [20–22]. FXR activation and inhibition in the liver and small intestine is known to regulate downstream genes that reduce high-density lipoprotein (HDL) cholesterol activity, reduce obesity, lower serum triglycerides, and maintain bile acid homeostasis [23–26].

Endogenous bile acids can generally be classified as hydrophobic, such as lithocholic acid (LCA) and deoxycholic acid (DCA), or hydrophilic, such as ursodeoxycholic acid (UDCA) and tauroursodeoxycholic acid (TUDCA) (Figure 1) [19,21,27–29]. The common primary bile acids, namely chenodeoxycholic acid (CDCA) and cholic acid (CA), are less hydrophobic than LCA and DCA but less hydrophilic than UDCA and TUDCA [30]. This classification underscores the importance of aqueous solubility in determining bile acid properties. In particular, the hydrophobic primary bile acids are initially toxic but are detoxified by liver enzymes to produce metabolites with higher water solubility [31]. The hydrophobic–hydrophilic balance of bile acids is crucial in bile acid homeostasis, as hydrophobic bile acids have been shown to induce inflammation, hepatocyte apoptosis, cytotoxicity, and cancer in gastrointestinal organs when exposed long term at high physiologic concentrations [32]. Hydrophilic bile acids, on the other hand, have been found to protect against cell death and exhibit anticancer effects, where prominence of effect depends on cell types [33–35]. Additional factors requiring consideration include solubility and membrane permeability, which are fundamental predictors of intestinal drug absorption and may be optimized to enhance the pharmacokinetic and clinical properties of synthetic agonists for drug discovery and development [36]. These factors are especially important in drug design since preclinical animal studies have revealed that systemic activation of bile acid pathways from rapid drug absorption results in off-target effects, such as pruritus and cardiovascular issues [37,38]. Increased doses of bile acids have also led to clinical cases of severe hepatotoxicity. These effects could be diminished by modulating intestinal absorption through hydroxylation to prevent bile acid accumulation in enterohepatic circulation [39]. As a result, improving bile acid hydrophilicity could reduce systemic side effects.

Despite the need to examine bile acid hydrophilicity, previous studies have primarily focused on modifying endogenous bile acids to improve potency and selectivity for TGR5 and/or FXR, rather than optimizing major fragments to improve hydrophilicity [40]. In this study, we reasoned that modification of the side chains of endogenous bile acids could enhance their hydrophilic properties to explore the development of new biological activity fragments of endogenous bile acids. The novel fragments were evaluated using luciferase-based reporter assays to elucidate their biological properties, and cell proliferation was determined by MTS assay. We applied our computational docking method to explore and explain the novel fragments–activity relationship. Considering the advantages of improved bile acid hydrophilicity, structurally modifying the side chain of bile acids may serve as an attractive strategy to design and optimize major fragments of endogenous bile acids.

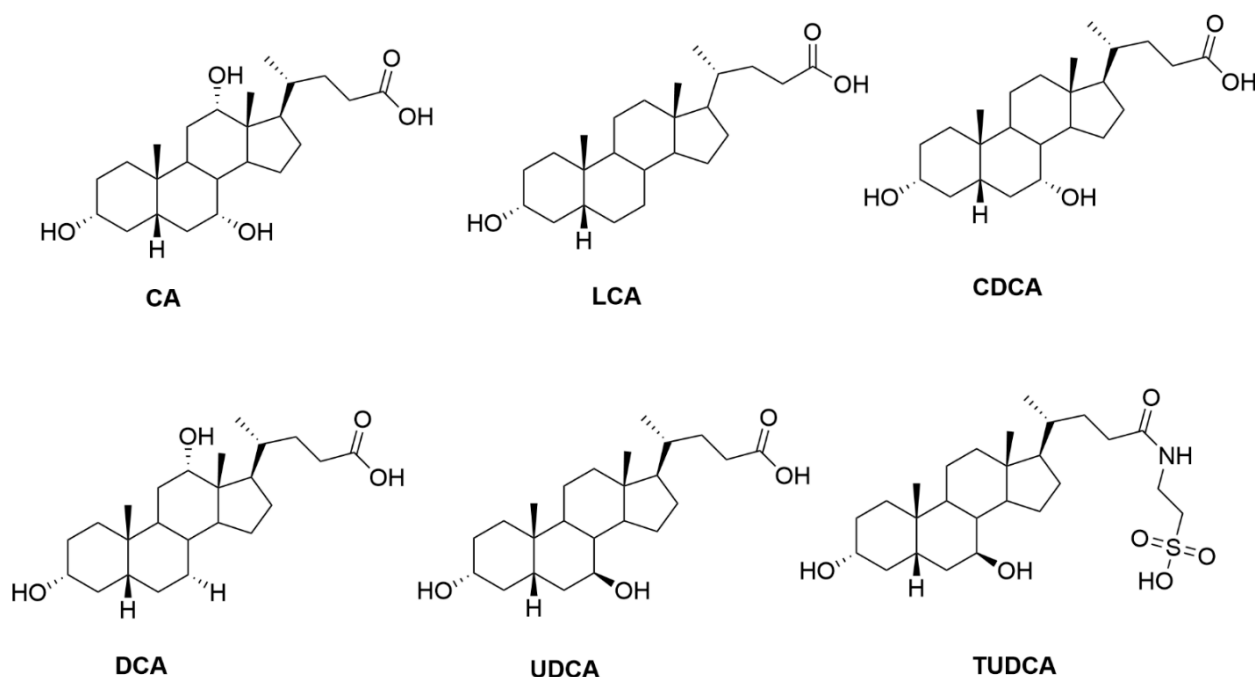


**Figure 1.** Chemical structures of endogenous bile acids that are TGR5 and/or FXR ligands.

## 2. Results and Discussion

### 2.1. A Novel Strategy to Design New Structure Fragments Based on LCA with Improved Hydrophilicity

Reports on modifying the side chains of endogenous bile acids for improving hydrophilicity are scarce. In fact, Wang et al. conducted the only modification study to date on 22-oxa-chenodeoxycholic acid (22-oxa-CDCA) [41]. However, they did not conduct any biological activity. Additionally, their synthesis method was limited. As introducing a polar “oxygen atom” has been an effective method to modify potent small molecule drugs, we hypothesized it would serve as an attractive starting point on the side chains for synthesizing novel bile acids. In the present study, we chose to design and optimize the major fragment of LCA, one of the most hydrophobic endogenous bile acids, by introducing a polar “oxygen atom” into the 22-position of the LCA side chain, then (i) either retaining the carboxylic acid group (**1a**) or replacing the carboxylic acid group with (ii) a diol group (**1b**) or (iii) a vinyl group (**1c**) (Figure 2). The logP values for compounds **1a–c** were calculated to be 3.93, 3.61, and 5.36, respectively. Compound **1a** (22-oxo-24-carboxylic acid-LCA) and compound **1b** (22-oxo-24,25-diol-LCA) demonstrated improved hydrophilic properties compared to LCA (3.93 and 3.61 vs. 5.30), while the logP value of compound **1c** (22-oxo-24-vinyl-LCA) was similar to that of LCA (5.36 vs. 5.30) as the control.

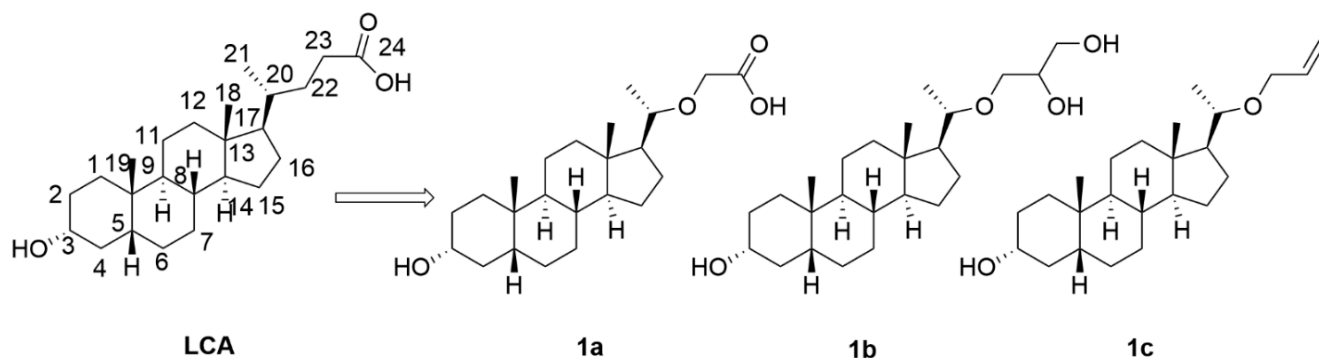


**Figure 2.** Strategy to design novel compounds **1a–1c** based on LCA.

Using our in-house-developed all-around docking method [42,43], we were able to predict the binding pocket and docking poses of LCA and its three analogs, **1a–1c**. According to Figure 3, LCA and its three analogs all preferred to bind at the activity site of the TGR5 protein with high docking scores, which is composed of residues of L71, L74, W75, Y89, P92, F96, S157, F161, Y240, T243, L244, S247, L266, and S270. Given the fairly high docking scores for all the compounds, syntheses of compounds **1a–1c** were performed consequently. However, a sub-pocket could also be formed by a specific network of hydrogen bonds between the side of bile acids and TGR5, which affected the compound's activity, as discussed in Section 2.4. Structure–Activity Relationship Analysis.

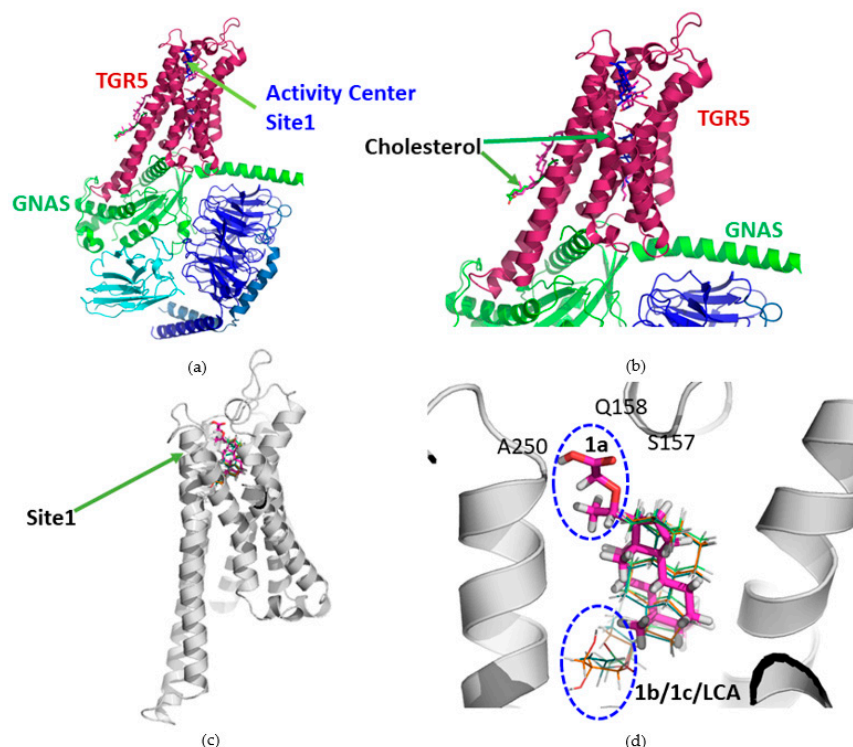


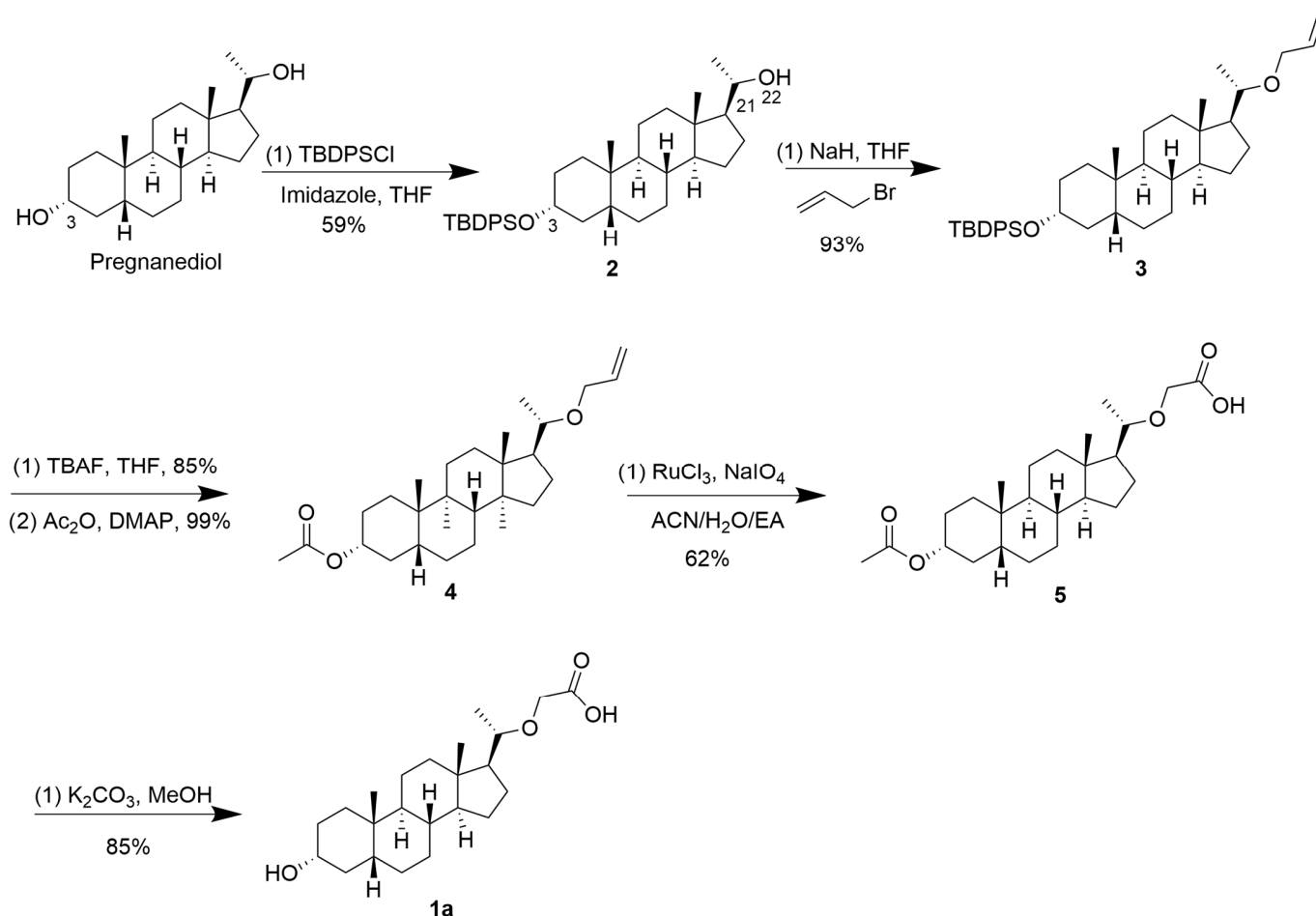
**Figure 3.** Activity center of TGR5 receptor and docking poses of LCA and its three analogs, **1a–1c**, in active center. (a) Protein TGR5 and its related activity center. (b) Magnification of TGR5 showing clear activity center. (c) LCA and its analogs **1a–1c** preferred to bind at the activity site of TGR5 protein. (d) Magnification of binding site of these analogs. Compounds LCA, **1b** and **1c** had very similar docking poses. Compound **1a** took an upside-down docking pose to form hydrogen bonds with S157, Q158, and A250 residues in TGR 5 protein.

## 2.2. Design and Synthesis of Compounds **1a–1c**

Design and synthesis of compounds **1a–1c** began with commercially available pregnanediol. Because of the differences in the steric hindrance of the two hydroxy groups on pregnanediol, the 3-hydroxy group on pregnanediol could be selectively protected by *tert*-Butyldiphenylchlorosilane (TBDPSCI) to obtain compound **2** with a 59% yield.

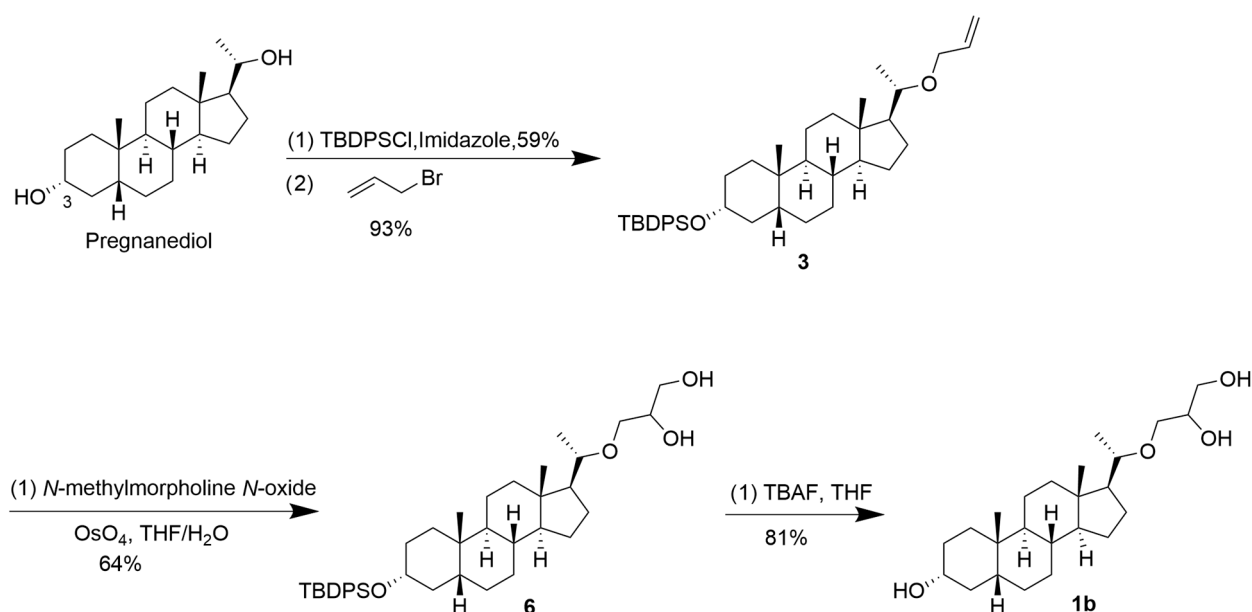
The synthesis route for compound **1a** initially involved a 3-step synthetic route with compound **2** as the starting material: (i) reaction with ethyl bromoacetate (22-position); (ii) deprotection of TBDPS (3-position); and (iii) hydrolysis of the ester group (22-position). Unfortunately, there was no reaction between compound **2** and ethyl bromoacetate; we tested the reaction under multiple conditions, including different reaction temperatures, bases (potassium carbonate, sodium hydride or *t*-butyl lithium), and solvents (acetonitrile, DMF, DMSO, and THF). The failed reaction was determined to be potentially due to the large steric hindrance between the hydroxyl group in compound **2** and ethyl bromoacetate. This prompted us to modify the synthesis route (Scheme 1) using the allyl group, since this group could be easily transformed to a carboxyl acid group under oxidizing conditions. We

experimented to develop a feasible synthesis method and compound **1a** was synthesized by inserting allyl group from compound **2**, deprotecting/protecting the 3-position hydroxyl group to obtain compound **4**, oxidizing the vinyl group of compound **4** to a carboxyl group by means of  $\text{RuCl}_3$  as a catalyst and  $\text{NaIO}_4$  as an oxidant, and removing the acetate group of compound **5** in a solution of potassium carbonate in methanol.



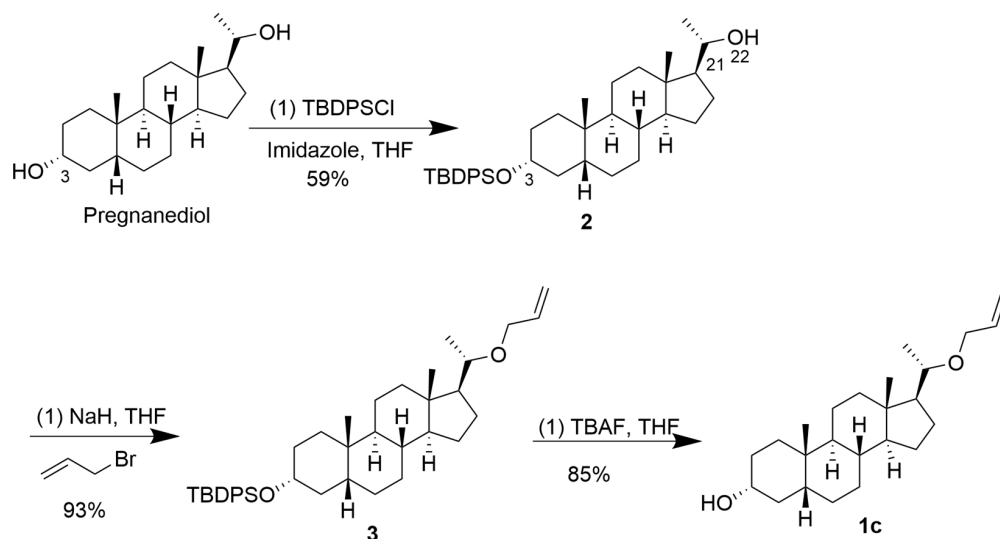
**Scheme 1.** Synthesis route of compound **1a**.

Meanwhile, compound **1b** was designed from compound **3** (Scheme 2). For this procedure, we followed a method discovered by Hoffmann in 1912 to achieve *cis*-dihydroxylation of alkenes [44]. However, the key step of this method was the cycloaddition of osmium tetroxide ( $\text{OsO}_4$ ) to the olefin, necessitating the use of stoichiometric amounts of the toxic and the expensive reagent  $\text{OsO}_4$ . To supplement this, Upjohn dihydroxylation was developed in 1976 and involves applying *N*-methylmorpholine *N*-oxide (NMO) as a stoichiometric re-oxidant for  $\text{OsO}_4$  [45]. Following Upjohn dihydroxylation, compound **3** was successfully oxidized to compound **6** without affecting the protected group TBDPS. Although ketone byproduct formation was reported for procedures following Upjohn dihydroxylation, we identified only a minute amount, which had no effect on purification, in the product. Finally, deprotection of TBDPS of compound **6** with TBAF afforded the target compound **1b** with 95% yield.



**Scheme 2.** Synthesis route of compound **1b**.

The synthesis route for compound **1c** is shown in Scheme 3. Classic conditions of  $\text{Ag}_2\text{O}$  and tetrabutylammonium iodide (TBAI) afforded compound **3**, but the reaction yield remained poor even when the reaction time was lengthened, and the temperature raised. The yield increased to 93% when we used sodium hydride as the base. Finally, deprotecting TBDPS with TBAF yielded the target compound **1c**.



**Scheme 3.** Synthesis route of compound **1c**.

### 2.3. Evaluated TGR5 Agonistic Activity and Cell Viability

To evaluate TGR5 agonistic activity, the novel compounds **1a–1c** and LCA were initially evaluated at concentrations of  $5\ \mu\text{M}$  via luciferase reporter assays based on our previous study to effectively activate TGR5 *in vitro* [40]. HEK293T cells were transfected with human TGR5 and cAMP-sensitive reporter plasmid pCRE-Luc and pCMV-Renilla as previously described [40]. At a low concentration, compound **1a** ( $1.97 \pm 0.07$ ) and compound **1b** ( $1.88 \pm 0.15$ ) exhibited agonist activity comparable to LCA ( $2.03 \pm 0.14$ ), whereas compound **1c** ( $1.25 \pm 0.04$ ) exhibited poor activity (Figure 4). The results showed that compounds **1a** and **1b** have no significantly different activity level than LCA, which

indicated that the **1a** and **1b** active structure combined with TGR5 at the same active site and sub-pocket as predicted in pervious section.

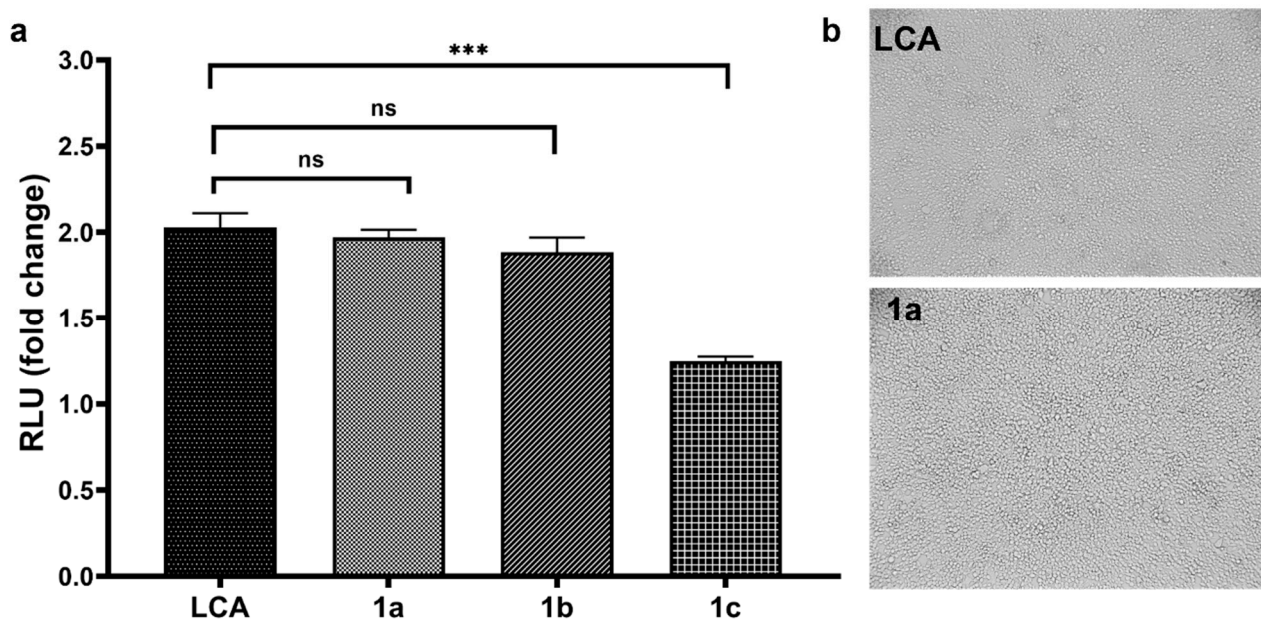


**Figure 4.** TGR5 agonistic activity of LCA and compounds **1a–1c** at 5  $\mu\text{M}$ . (a) Data are presented as mean  $\pm$  SE from  $n = 3$  replicates. Bioactivity was compared between groups using unpaired  $t$ -tests. ns: no significance ( $p > 0.05$ ); \*\*\*  $p < 0.001$ . (b) The representative images of HEK293T cells under treatment with 5  $\mu\text{M}$  LCA and 5  $\mu\text{M}$  compound **1a**. RLU, relative luciferase units.

We determined the changes in cAMP elicited by these LCA derivatives after binding to the TGR5 in order to determine their relative  $\text{EC}_{50}$  values. Compounds **1a** ( $\text{EC}_{50} = 4.688 \mu\text{M}$ ) and **1b** ( $\text{EC}_{50} = 21.45 \mu\text{M}$ ) displayed comparable activity to LCA ( $\text{EC}_{50} = 13.57 \mu\text{M}$ ). However, **1c** had almost no improved potency compared to LCA. Compound **1a** had the lowest  $\text{EC}_{50}$  tested among the compounds, and two reasons might mainly be attributed to this. First, the lower  $\text{EC}_{50}$  of **1a** than LCA may be due to the improved hydrophilicity with the polar oxygen atom added. The improved hydrophilicity may result in prolonged absorption and a higher affinity to TGR5. This can prevent the bile acids from binding the uninterested organs. The efficiency increases as the hydrophilicity increases, yet more examinations still need to be performed to verify the hypothesis. Second, compound **1a** maintains the original carboxylic acid structure as LCA. It preserves the maximum similar structure as far as possible. The other two compounds changed the side chain attached to 22-position to a diol group and a vinyl group correspondingly. The change in the original structure may lead to a decrease in efficiency. Additionally, we observed a non-linear relationship when measuring the  $\text{EC}_{50}$  value for three compounds: the efficiency does not increase at a constant rate as the dosage increases. Other studies on GTR5 agonists also shared the common problem that might be due to the limited absorption [46,47].

In the present study, HEK 293T cells were treated by compounds **1a–c** and LCA concentrations from 0 to 25  $\mu\text{M}$ . Cell viability was measured using the MTS assay. The findings revealed no statistically significant difference in cell viability across the range of 0–25  $\mu\text{M}$ . This suggests that new bile acid structures **1a–1c**, under the 25  $\mu\text{M}$  range, did not shown any sign of toxicity. The MTS assay results provided strong evidence that indicated that the increased activities, from pervious luciferase assay results, of compounds are independent of the toxicity within the specific 0 to 25  $\mu\text{M}$  range. This study provides an encouraging outlook that the newly modified structures have a favorable safety profile with improved efficiency. However, in order to comprehensively analyze the implications of these results and ascertain the safety and effectiveness of the three compounds across multiple environments, further studies and evaluations are imperative.





Previous studies have developed different methods to modify non-bile-acid TGR5 agonists to optimize intestinal targeting and reduce systemic side effects. The incorporation of a large, polar group in synthetic TGR5 agonists by Lasalle et al. reduced intestinal absorption and increased intestine-specific oral drug delivery [49]. The lead compound improved glucose tolerance in a murine model of obesity and insulin resistance. Another study incorporated polar functional groups to prepare a TGR5 agonist with low absorbance and decreased off-target activation of the gallbladder [50]. Furthermore, a potent gut-restricted TGR5 agonist demonstrated minimal gallbladder-related side effects in mice [51]. OL3, another TGR5 agonist with a hydrophilic side chain, effectively lowered blood glucose without gallbladder filling [52]. However, these studies have focused on non-bile-acid-derived synthetic molecules. In this study, we report the development of compounds **1a** and **1b** from the endogenous bile acid LCA through a novel methodology of introducing polar groups containing an oxygen base and retaining or modifying the carboxylic acid group. It was reported that increasing hydrophilicity could potentially limit intestinal permeability and reduce the side effects of LCA and its derivatives, which is particularly beneficial given that LCA is the most hydrophobic endogenous bile acid [53]. Furthermore, bile acids and derivatives beyond LCA may also benefit from a high topological polar surface due to the reduction in adverse effects from off-target binding [54], such as obeticholic acid (OCA), CDCA, and TUDCA, which have relatively hydrophobic bile acids. Current modifications of these compounds do not focus on their side chain. With the strategy we developed to obtain new bile acid analogs with improved hydrophilicity and comparable binding activity (**1a** and **1b**), bile acids demonstrating clinical potential could conceivably undergo similar permeability modifications to potentially reduce systemic activation and clinical side effects.

### 3. Materials and Methods

All reagents and chemicals were purchased from commercial suppliers and used without further purification unless otherwise stated.  $^1\text{H}$  and  $^{13}\text{C}$  spectra were recorded at Bruker 700 and 175 MHz, respectively, and the chemical shifts for  $^1\text{H}$ -NMR and  $^{13}\text{C}$ -NMR were referenced as tetramethylsilane (TMS) via residual solvent signals. The resonance patterns are indicated as follows: s, singlet; d, doublet; t, triplet; q, quartet; m, multiplet; dd, doublet of doublets; and dt, doublet of triplets. The coupling constants ( $J$ ) are reported in Hz. Mass spectra were obtained on an Agilent Infinitylab mass spectrometer equipped with an ESI source operated in positive mode or negative mode. Flash column chromatography was performed over silica gel of 200–300 mesh.

#### 3.1. Chemistry

(1S)-1-((3R,10S,13S)-3-((Tert-butyl)diphenylsilyloxy)-10,13-dimethylhexadecahydro-1H-cyclopenta[ $\alpha$ ]phenanthren-17-yl)ethan-1-ol (**2**). To a solution of (3R,10S,13S)-17-((S)-1-hydroxyethyl)-10,13-dimethylhexadecahydro-1H-cyclopenta[ $\alpha$ ]phenanthren-3-ol (Pregnenediol) (500 mg, 1.6 mmol, 1 Eq) and imidazole (325 mg, 3 Eq) in DCM (100 mL) at room temperature under nitrogen atmosphere, *tert*-Butyl(chloro)diphenylsilyl (650 mg, 1.2 Eq) was added. After 1 h, the reaction mixture was diluted with water (100 mL). The organic phase was separated, and the aqueous phase was extracted with DCM ( $3 \times 100$  mL). The organic phases were then combined and washed with water ( $3 \times 100$  mL) and brine ( $2 \times 100$  mL) and dried with sodium sulfate. The organic solvent was removed under reduced pressure. The crude product **2** was purified by silica gel flash column chromatography with DCM elution to furnish compound **2** as a sticky oil (525 mg, 59% yield).  $^1\text{H}$ -NMR (700 MHz,  $\text{CDCl}_3$ ):  $\delta$  7.67–7.69 (m, 4H), 7.40–7.42 (m, 2H), 7.35–7.38 (m, 4H), 3.64–3.40 (m, 1H), 3.60–3.63 (m, 1H), 1.81–1.92 (m, 3H), 1.7–1.8 (m, 1H), 1.45–1.71 (m, 5H), 1.32–1.46 (m, 6H), 1.12–1.36 (m, 10H), 1.05 (s, 9H), 0.82 (s, 3H), 0.71–0.76 (m, 1H), 0.63 (s, 3H).

(((3R,10S,13S)-17-((S)-1-(allyloxy)ethyl)-10,13-dimethylhexadecahydro-1H-cyclopenta[ $\alpha$ ]phenanthren-3-yl)oxy)(*tert*-butyl)diphenylsilyl (**3**). To a suspension of sodium hydride (NaH) in THF (4 mL)

in a sealed tube at room temperature compound 2 (350 mg, 0.63 mmol) in THF (2 mL) was added dropwise. The mixture was stirred at room temperature for 30 min. Then, allyl bromide (150 mg, 2 Eq) was added to the above reaction mixture. The reaction mixture was stirred and heated at 110 °C for 8 h. The reaction was quenched with water (20 mL) at room temperature. The reaction mixture was then extracted with ethyl acetate (3 × 20 mL), dried over sodium sulfate, and filtered and concentrated under reduced pressure. The crude product was purified by silica gel flash column chromatography with hexane and ethyl acetate (*v/v*, 50:1) as eluents to afford compound 3 as a white solid (350 mg, 93% yield). <sup>1</sup>H-NMR (700 MHz, CDCl<sub>3</sub>): δ 7.67–7.69 (m, 4H), 7.40–7.42 (m, 2H), 7.35–7.38 (m, 4H), 5.89–5.94 (m, 1H), 5.25 (d, *J* = 16.8 Hz, 1H), 5.12 (d, *J* = 10.5 Hz, 1H), 4.06–4.09 (m, 1H), 3.80–3.84 (m, 1H), 3.60–3.63 (m, 1H), 3.28–3.63 (m, 1H), 1.91–1.98 (m, 1H), 1.82–1.86 (m, 2H), 1.72–1.76 (m, 2H), 1.31–1.55 (m, 13H), 1.16 (d, *J* = 6.3 Hz, 3H), 1.09–1.15 (m, 3H), 1.05 (s, 9H), 0.81 (s, 3H), 0.73 (m, 1H), 0.61 (s, 3H).

(3*R*,10*S*,13*S*)-17-((*S*)-1-(Allyloxy)ethyl)-10,13-dimethylhexadecahydro-1*H*-cyclopenta[α]phenanthren-3-ol (**1c**). To a solution of compound 3 (350 mg, 0.59 mmol) in THF (3 mL) at room temperature, TBAF was added (3 mL, 1 M, in THF). The resulting mixture was stirred at room temperature overnight. The solvent was then removed under reduced pressure, and the residue was purified by silica gel flash column chromatography with hexane and ethyl acetate as eluents (*v/v*, 5:1) to furnish compound 1c as a white solid (180 mg, 85% yield). <sup>1</sup>H-NMR (700 MHz, CDCl<sub>3</sub>): δ 5.87–5.93 (m, 1H), 5.24 (d, *J* = 16.8 Hz, 1H), 5.10 (d, *J* = 10.5 Hz, 1H), 4.05–4.08 (m, 1H), 3.80–3.83 (m, 1H), 3.60–3.63 (m, 1H), 3.27–3.30 (m, 1H), 1.91–1.96 (m, 1H), 1.81–1.86 (m, 2H), 1.73–1.79 (m, 2H), 1.65–1.69 (m, 1H), 1.46–1.54 (m, 2H), 1.34–1.43 (m, 7H), 1.17–1.34 (m, 3H), 1.15 (d, *J* = 6.3 Hz, 3H), 1.04–1.13 (m, 4H), 0.96–0.99 (m, 1H), 0.91 (s, 3H), 0.62 (s, 3H). <sup>13</sup>C-NMR (175 MHz, CDCl<sub>3</sub>), δ 136.25, 116.60, 78.24, 72.36, 69.79, 57.63, 56.86, 42.60, 40.99, 39.82, 36.91, 36.06, 35.87, 31.02, 30.99, 27.67, 26.93, 26.90, 26.86, 24.61, 23.85, 21.07, 21.04, 19.69, 13.10. MS for C<sub>24</sub>H<sub>40</sub>O<sub>2</sub> calculated: *m/z* 383.3 (M + Na)<sup>+</sup>; found: 383.3.

(3*R*,10*S*,13*S*)-17-((*S*)-1-(Allyloxy)ethyl)-10,13-dimethylhexadecahydro-1*H*-cyclopenta[α]phenanthren-3-yl acetate (**4**). To a solution of (3*R*,10*S*,13*S*)-17-((*S*)-1-(allyloxy)ethyl)-10,13-dimethylhexadecahydro-1*H*-cyclopenta[α]phenanthren-3-ol, **1c** (180 mg, 0.5 mmol) and 4-Dimethylaminopyridine (DMAP) (132 mg, 1.5 Eq) in dichloromethane (DCM) (6 mL) at room temperature, acetic anhydride (60 mg, 1.2 Eq) was added. The resulting mixture was stirred at room temperature for 4 h. The solvent was then removed under reduced pressure and the residue was purified by silica gel flash column chromatography with hexane and ethyl acetate as elution (*v/v*, 20:1) to furnish compound 4 as a viscous oil (200 mg, 99% yield). <sup>1</sup>H-NMR (700 MHz, CDCl<sub>3</sub>): δ 5.85–5.89 (m, 1H), 5.23 (d, *J* = 16.8 Hz, 1H), 5.09 (d, *J* = 10.5 Hz, 1H), 4.67–4.71 (m, 1H), 4.03–4.06 (m, 1H), 3.78–3.81 (m, 1H), 3.24–3.28 (m, 1H), 2.0 (s, 3H), 1.89–1.94 (m, 1H), 1.77–1.86 (m, 4H), 1.64–1.67 (m, 2H), 1.55–1.59 (m, 1H), 1.45–1.54 (m, 2H), 1.34–1.43 (m, 8H), 1.17–1.23 (m, 2H), 1.13 (d, *J* = 6.3 Hz, 3H), 1.02–1.08 (m, 5H), 0.96–1.02 (m, 1H), 0.90 (s, 3H), 0.60 (s, 3H).

2-((1*S*)-1-((3*R*,10*S*,13*S*)-3-Acetoxy-10,13-dimethylhexadecahydro-1*H*-cyclopenta[α]phenanthren-17-yl) ethoxy) acetic acid (**5**). Compound 4 (200 mg, 0.5 mmol) and RuCl<sub>3</sub> (10 mg, 0.1 Eq) were dissolved in a mixed solvent of acetonitrile (4 mL), water (6 mL) and ethyl acetate (4 mL) at room temperature, and then NaIO<sub>4</sub> (560 mg, 4 Eq) was added. The resulting mixture was stirred at room temperature overnight. The reaction mixture was then diluted with water (60 mL) and ethyl acetate (60 mL). The aqueous phase was separated and extracted with ethyl acetate (3 × 60 mL). The organic phases were combined and washed with water (2 × 30 mL) and brine (2 × 30 mL), followed by drying using sodium sulfate. The solvents were removed under reduced pressure and the residue was purified by silica gel flash column chromatography with dichloromethane and methanol as elution (*v/v*, 25:1) to furnish compound 5 as a viscous oil (130 mg, 62% yield). <sup>1</sup>H-NMR (700 MHz, CDCl<sub>3</sub>): δ 4.58–4.61 (m, 1H), 4.11 (d, *J* = 9.1 Hz, 1H), 3.93 (d, *J* = 16.1 Hz, 1H), 3.40–3.45 (m,

1H), 2.0 (s, 3H), 1.89–1.94 (m, 1H), 1.77–1.86 (m, 4H), 1.61–1.69 (m, 2H), 1.35–1.56 (m, 9H), 1.21–1.27 (m, 2H), 1.19 (d,  $J = 6.3$  Hz, 3H), 1.06–1.17 (m, 4H), 0.96–1.02 (m, 1H), 0.91 (s, 3H), 0.62 (s, 3H).

2-((1S)-1-((3R,10S,13S)-3-Hydroxy-10,13-dimethylhexadecahydro-1H-cyclopenta[ $\alpha$ ]phenanthren-17-yl) ethoxy) acetic acid (**1a**). To a solution of compound **5** (130 mg, 0.31 mmol) in MeOH (10 mL) at room temperature  $K_2CO_3$  (1.07 g in 0.5 mL water, 25 Eq) was added aq. The resulting mixture was stirred for 4 h. The reaction mixture was then quenched with water (50 mL) and adjusted to a pH of 2 with 3M hydrochloric acid. The white precipitate was extracted with ethyl acetate ( $3 \times 50$  mL). The organic phases from each of the extractions were combined and dried with sodium sulfate. The solvent was removed under reduced pressure, and the residue was purified by silica gel flash column chromatography with dichloromethane and methanol elution ( $v/v$ , 25:1) to produce compound **1a** as a white solid (100 mg, 85% yield).  $^1H$ -NMR (700 MHz,  $CDCl_3$ ):  $\delta$  4.12 (d,  $J = 16.1$  Hz, 1H), 3.92 (d,  $J = 16.1$  Hz, 1H), 3.59–3.64 (m, 1H), 3.42–3.46 (m, 1H), 1.89–1.94 (m, 1H), 1.77–1.86 (m, 2H), 1.71–1.79 (m, 2H), 1.63–1.66 (m, 3H), 1.45–1.61 (m, 3H), 1.35–1.43 (m, 6H), 1.22–1.32 (4H), 1.06–1.23 (m, 7H), 0.94–0.98 (m, 1H), 0.90 (s, 3H), 0.62 (s, 3H).  $^{13}C$ -NMR (175 MHz,  $CDCl_3$ ):  $\delta$  80.94, 72.34, 65.90, 57.06, 56.77, 42.51, 40.91, 39.71, 36.84, 36.00, 35.80, 30.94, 27.59, 26.93, 26.87, 24.56, 23.81, 21.02, 19.53, 13.12. MS for  $C_{23}H_{38}O_4$  calculated:  $m/z$  377.3 ( $M - H$ )<sup>-</sup>; found: 377.3.

3-((1S)-1-((3R,10S,13S)-3-((Tert-butyl)diphenylsilyl) oxy)-10,13-dimethylhexadecahydro-1H-cyclopenta[ $\alpha$ ]phenanthren-17-yl) ethoxy)propane-1,2-diol (**6**). (((3R,10S,13S)-17-((S)-1-(allyloxy) ethyl)-10,13-dimethylhexadecahydro-1H-cyclopenta[ $\alpha$ ]phenanthren-3-yl) oxy)(tert-butyl) diphenylsilane, **3** (200 mg, 0.34 mmol, 1 Eq) and  $OsO_4$  (4.5 mg, 0.05 Eq) were dissolved in a mixture solvent of THF (1 mL) and water (1 mL), and then *N*-methylmorpholine *N*-oxide (80 mg, 0.68 mmol, 2 Eq) was added at room temperature. The resulting mixture was stirred at room temperature overnight. The reaction mixture was then diluted with water (30 mL) and ethyl acetate (30 mL). The aqueous phase was separated and extracted with ethyl acetate ( $3 \times 30$  mL). The organic phases were combined and washed with water ( $2 \times 30$  mL) and brine ( $2 \times 30$  mL), followed by drying with sodium sulfate. The solvent was removed under reduced pressure, and the residue was purified by silica gel flash column chromatography with dichloromethane and methanol as elution (20:1) to furnish compound **6** as a viscous oil (138 mg, 64% yield).  $^1H$ -NMR (700 MHz,  $CDCl_3$ ):  $\delta$  7.65–7.67 (m, 4H), 7.37–7.41 (m, 2H), 7.33–7.35 (m, 4H), 3.77–3.79 (m, 1H), 3.67–3.72 (m, 1H), 3.55–3.64 (m, 2H), 3.35–3.42 (m, 1H), 3.27–3.31 (m, 1H), 3.24–3.26 (m, 1H), 2.58 (dd,  $J = 19.6, 5.6$  Hz, 1H), 2.19 (d,  $J = 19.6$  Hz, 1H), 1.81–1.90 (m, 2H), 1.71–1.79 (m, 2H), 1.68–1.71 (m, 1H), 1.55–1.61 (m, 5H), 1.35–1.51 (m, 7H), 1.12–1.21 (m, 8H), 1.03 (s, 9H), 0.79 (s, 3H), 0.58–0.62 (m, 1H), 0.59 (s, 3H).

3-((1S)-1-((3R,10S,13S)-3-Hydroxy-10,13-dimethylhexadecahydro-1H-cyclopenta[ $\alpha$ ]phenanthren-17-yl)ethoxy)propane-1,2-diol (**1b**). To a solution of compound **6** (138 mg, 0.22 mmol, 1 Eq) in THF (12 mL), TBAF was added at room temperature (2 mL, 1 M in THF). The resulting mixture was stirred at room temperature overnight. The reaction mixture was diluted with water (30 mL) and extracted with ethyl acetate (30 mL). The aqueous phase was separated and extracted with ethyl acetate ( $3 \times 30$  mL). The organic phases were combined and washed with water ( $2 \times 30$  mL) and brine ( $2 \times 30$  mL), followed by drying with sodium sulfate. The solvent was removed under reduced pressure. The residue was purified by silica gel flash column chromatography with dichloromethane and methanol elution (20:1) to furnish compound **1b** as a viscous oil (70 mg, 81% yield).  $^1H$ -NMR (700 MHz,  $CDCl_3$ ):  $\delta$  3.77–3.79 (m, 1 H), 3.67–3.72 (m, 1 H), 3.59–3.64 (m, 2 H), 3.35–3.42 (m, 1 H), 3.27–3.31 (m, 1 H), 3.24–3.26 (m, 1 H), 2.58 (dd,  $J = 19.6, 5.6$  Hz, 1 H), 2.19 (d,  $J = 19.6$  Hz, 1 H), 1.81–1.91 (m, 3 H), 1.71–1.79 (m, 2 H), 1.58–1.66 (m, 2 H), 1.45–1.58 (m, 6 H), 1.35–1.43 (m, 5 H), 1.02–1.31 (m, 8 H), 0.92–0.98 (m, 1 H), 0.90 (s, 3 H), 0.61 (s, 3 H).  $^{13}C$ -NMR (175 MHz,

CDCl<sub>3</sub>),  $\delta$  77.69, 70.32, 69.10, 68.63, 63.16, 55.49, 54.76, 40.55, 38.96, 37.75, 34.93, 34.02, 33.84, 29.01, 25.64, 24.92, 24.84, 24.73, 24.70, 22.59, 21.83, 19.03, 17.51, 11.16. MS for C<sub>24</sub>H<sub>42</sub>O<sub>4</sub> calculated:  $m/z$  417.3 (M + Na)<sup>+</sup>; found: 417.3.

### 3.2. Biological Activity-Luciferase Reporter Gene Assays and Survival/Proliferation Assay

**Cell culture.** HEK293T cells (ATCC, Manassas, VA, USA) were constructed to the TGR5-overexpressing HEK293T cells in our team as previously reported [38]. The cells were cultured in high-glucose Dulbecco's modified Eagle's medium (DMEM; Thermo Fisher, Pittsburg, PA, USA) with L-glutamine supplemented with 10% (vol/vol) heat-inactivated fetal bovine serum (Atlas Biologicals, Fort Collins, CO, USA) and 1% penicillin-streptomycin (Thermo Fisher). TGR5-overexpressing HEK293T cells were maintained in G418 (Thermo Fisher)-containing media until plating. Cells were seeded onto 24-well plates (5 × 10<sup>5</sup> cells/well) 24 h before transfection.

**Luciferase reporter gene assays.** To evaluate TGR5 agonistic activity, HEK293T cells were transfected with human TGR5 expression vector, pCRE-Luc reporter vector, and pCMV-Renilla luciferase vector as an internal control for normalization of transfection efficiency. Plasmids were complexed with PEI (Promega, Madison, WI, USA) in OptiMEM (Invitrogen, Carlsbad, CA, USA). After 18 h, cells were treated with vehicle (DMSO) and the appropriate ligand as indicated (5  $\mu$ M). Luciferase activities were assayed after 6 h using Luciferase Assay System (Promega) and an MLX luminometer (Dynex Technologies, Chantilly, VA, USA).

**Effective Concentrations (EC<sub>50</sub>) of 50% and Efficacy Determination.** Assays were performed by the above assay. To evaluate TGR5 activity of compounds, cells were transfected with 100 ng pCRE-luc reporter, along with pCMV-Renilla (10 ng) as an internal control, for normalization of transfection efficiency. Plasmids were complexed with 2 mL of OptiMEM (Invitrogen, Carlsbad, CA, USA), and cells were transfected for 18 h. The following day, cells were treated with vehicle and compound with increasing concentrations of 0.01, 0.1, 1.0, 10, and 100  $\mu$ M. Luciferase was assayed 6 h later using Luciferase Assay System (Promega) reagents.

**Survival/Proliferation Assay.** Cell proliferation was determined by MTS assay, which was conducted with the Cell Titer 96 Aqueous Cell Proliferation Kit (Promega). To test IC<sub>50</sub>, 3 × 10<sup>3</sup> HEK 293T cells cultured in a 96-well plate were treated with increasing concentrations of compounds **1a–1c** and LCA for 48 h. After adding the MTS reagents, the plate was incubated for 3 h in a humidified, 37 °C incubator supplemented with a 5% CO<sub>2</sub> atmosphere. The plate was read with a 96-well spectrometer using a 490 nm filter. The half-maximal inhibitory concentration (IC<sub>50</sub>) was described as the drug concentration that induced viability decrease by 50%.

### 3.3. Computational Modeling

The TGR5 protein structure was downloaded from the RCSB Protein Data Bank (PDB id 7cfm [55]). We used our in-house-developed all-around docking (AAD) [42,43] method to dock LCA and its 3 analogs **1a–1c** onto the whole surface of the TGR5 protein to automatically search for the best binding pocket and docking pose of each compound. The protein interaction analysis was performed using our in-house-developed LiAn (Ligand Interfaces Analysis) [56] program, which could estimate and display protein–ligand or protein–protein interactions (including hydrogen bond, salt–bridge, water–bridge,  $\pi$ –interactions, hydrophobic interactions, halogen bond, etc.) for single-protein structures or massive structures from molecular dynamics simulations. The protein structure figure was produced using PyMoL (The PyMoL Molecular Graphics System, Version 2.0 Schrödinger, LLC, San Diego, CA, USA). The two-dimensional interaction diagram was produced using Schrödinger Maestro software.

#### 4. Conclusions

In short, we successfully characterized a novel strategy for the development of bioactivity fragments based on the endogenous bile acid LCA to modulate the activity of LCA-related receptor TGR5. We developed a feasible strategy to synthesize these fragments. Three novel analogs, **1a–1c**, and LCA were evaluated using luciferase reporter gene assays and MTS assays. The initial results indicated that compounds **1a** and **1b** improved the hydrophilicity of the fragments and displayed agonist activities for TGR5. Our computational modeling supported this result by showing that compounds **1a** and **1b** could form more effective hydrogen bonds with hydrophilic residues. To the best of our knowledge, these lead compounds have not been previously reported in the literature. We hypothesize that this method could be applied to modify other bile acids to potentially improve hydrophilicity. Currently, we are in the process of evaluating the biological activity of these novel structure fragments.

**Author Contributions:** J.P. and M.F.: Study design, Methodology, Analysis, and Manuscript Editing; L.A.H., K.X.H., R.Y. and H.Z.: Analysis, Computational Analysis, Manuscript Draft Preparation, and Manuscript Editing; H.L.: Computational Analysis; Y.W., S.X. and A.A.: Methodology and Analysis; J.X.: Study design; D.A.H. and F.K.: Conceptualization and Investigation; W.H.: Conceptualization, Investigation, Study Design, Analysis, Methodology, and Funding Acquisition; J.L.: Conceptualization, Investigation, Study Design, Manuscript Draft Preparation, Analysis, Methodology, Manuscript Editing, and Funding Acquisition. All authors have read and agreed to the published version of the manuscript.

**Funding:** This work was supported by Wanek Family Project for Type 1 Diabetes (Grant No. 2011440 to J.L.), the Oxnard Foundation (Grant No. 50214-2012049 to J.L.), The National Institutes of Health grants (R01DK124627 to W.H. and COH P30CA33572 to COH).

**Institutional Review Board Statement:** Not applicable.

**Informed Consent Statement:** Not applicable.

**Data Availability Statement:** Not applicable.

**Acknowledgments:** We acknowledge financial support for this work from Wanek Family Project for Type 1 Diabetes (2011440). We acknowledge Zhipeng Fang obtained microscopic observation images of HEK293T cells under treatment. We acknowledge Jiaqi Chen and Zhixuan Li for revising and editing the manuscript.

**Conflicts of Interest:** The authors declare no conflict of interest.

**Sample Availability:** Not applicable.

#### References

1. Keitel, V.; Kubitz, R.; Haussinger, D. Endocrine and paracrine role of bile acids. *World J. Gastroenterol.* **2008**, *14*, 5620–5629. [[CrossRef](#)] [[PubMed](#)]
2. Hansen, M.; Scheltema, M.J.; Sonne, D.P.; Hansen, J.S.; Sperling, M.; Rehfeld, J.F.; Holst, J.J.; Vilsboll, T.; Knop, F.K. Effect of chenodeoxycholic acid and the bile acid sequestrant colestevlam on glucagon-like peptide-1 secretion. *Diabetes Obes. Metab.* **2016**, *18*, 571–580. [[CrossRef](#)] [[PubMed](#)]
3. Zheng, X.J.; Chen, T.L.; Jiang, R.Q.; Zhao, A.H.; Wu, Q.; Kuang, J.L.; Sun, D.N.; Ren, Z.X.; Li, M.C.; Zhao, M.; et al. Hyocholic acid species improve glucose homeostasis through a distinct TGR5 and FXR signaling mechanism. *Cell Metab.* **2021**, *33*, 791–803.e7. [[CrossRef](#)] [[PubMed](#)]
4. Zhuang, L.; Ding, W.; Zhang, Q.; Ding, W.; Xu, X.; Yu, X.; Xi, D. TGR5 Attenuated Liver Ischemia-Reperfusion Injury by Activating the Keap1-Nrf2 Signaling Pathway in Mice. *Inflammation* **2021**, *44*, 859–872. [[CrossRef](#)]
5. Howlett-Prieto, Q.; Langer, C.; Rezanian, K.; Soliven, B. Modulation of immune responses by bile acid receptor agonists in myasthenia gravis. *J. Neuroimmunol.* **2020**, *349*, 577397. [[CrossRef](#)]
6. Wu, L.; Feng, J.; Li, J.; Yu, Q.; Ji, J.; Wu, J.; Dai, W.; Guo, C. The gut microbiome-bile acid axis in hepatocarcinogenesis. *Biomed. Pharmacother.* **2021**, *133*, 111036. [[CrossRef](#)]
7. Trah, J.; Arand, J.; Oh, J.; Pagerols-Raluy, L.; Trochimiuk, M.; Appl, B.; Heidelberg, H.; Vincent, D.; Saleem, M.A.; Reinshagen, K.; et al. Lithocholic bile acid induces apoptosis in human nephroblastoma cells: A non-selective treatment option. *Sci. Rep.* **2020**, *10*, 20349. [[CrossRef](#)]

8. Wu, H.H.; Yu, N.N.; Wang, X.; Yang, Y.N.; Liang, H. Tauroursodeoxycholic acid attenuates neuronal apoptosis via the TGR5/SIRT3 pathway after subarachnoid hemorrhage in rats. *Biol. Res.* **2020**, *53*, 56. [[CrossRef](#)]
9. Ito, K.; Okumura, A.; Takeuchi, J.S.; Watashi, K.; Inoue, R.; Yamauchi, T.; Sakamoto, K.; Yamashita, Y.; Iguchi, Y.; Une, M.; et al. Dual Agonist of Farnesoid X Receptor and Takeda G Protein-Coupled Receptor 5 Inhibits Hepatitis B Virus Infection In Vitro and In Vivo. *Hepatology* **2021**, *74*, 83–98. [[CrossRef](#)]
10. Yang, J.; Palmiotti, A.; Kuipers, F. Emerging roles of bile acids in control of intestinal functions. *Curr. Opin. Clin. Nutr. Metab. Care* **2021**, *24*, 127–133. [[CrossRef](#)]
11. Sorrentino, G.; Perino, A.; Yildiz, E.; El Alam, G.; Sleiman, M.B.; Gioiello, A.; Pellicciari, R.; Schoonjans, K. Bile Acids Signal via TGR5 to Activate Intestinal Stem Cells and Epithelial Regeneration. *Gastroenterology* **2020**, *159*, 956–968.e8. [[CrossRef](#)] [[PubMed](#)]
12. Song, M.; Yang, Q.; Zhang, F.L.; Chen, L.; Su, H.; Yang, X.H.; He, H.W.; Liu, F.F.; Zheng, J.S.; Ling, M.F.; et al. Hyodeoxycholic acid (HDCA) suppresses intestinal epithelial cell proliferation through FXR-PI3K/AKT pathway, accompanied by alteration of bile acids metabolism profiles induced by gut bacteria. *Faseb J.* **2020**, *34*, 7103–7117. [[CrossRef](#)] [[PubMed](#)]
13. Wang, J.; Zhang, J.; Lin, X.; Wang, Y.; Wu, X.; Yang, F.; Gao, W.; Zhang, Y.; Sun, J.; Jiang, C.; et al. DCA-TGR5 signaling activation alleviates inflammatory response and improves cardiac function in myocardial infarction. *J. Mol. Cell. Cardiol.* **2021**, *151*, 3–14. [[CrossRef](#)] [[PubMed](#)]
14. Shen, H.; Ding, L.; Baig, M.; Tian, J.; Wang, Y.; Huang, W. Improving glucose and lipids metabolism: Drug development based on bile acid related targets. *Cell Stress* **2021**, *5*, 1–18. [[CrossRef](#)] [[PubMed](#)]
15. Watanabe, M.; Houten, S.M.; Matakai, C.; Christoffolete, M.A.; Kim, B.W.; Sato, H.; Messaddeq, N.; Harney, J.W.; Ezaki, O.; Kodama, T.; et al. Bile acids induce energy expenditure by promoting intracellular thyroid hormone activation. *Nature* **2006**, *439*, 484–489. [[CrossRef](#)] [[PubMed](#)]
16. Pols, T.W.; Nomura, M.; Harach, T.; Sasso, G.L.; Oosterveer, M.H.; Thomas, C.; Rizzo, G.; Gioiello, A.; Adorini, L.; Pellicciari, R.; et al. TGR5 activation inhibits atherosclerosis by reducing macrophage inflammation and lipid loading. *Cell Metab.* **2011**, *14*, 747–757. [[CrossRef](#)]
17. Sasaki, T.; Watanabe, Y.; Kuboyama, A.; Oikawa, A.; Shimizu, M.; Yamauchi, Y.; Sato, R. Muscle-specific TGR5 overexpression improves glucose clearance in glucose-intolerant mice. *J. Biol. Chem.* **2021**, *296*, 100131. [[CrossRef](#)]
18. Maruyama, T.; Miyamoto, Y.; Nakamura, T.; Tamai, Y.; Okada, H.; Sugiyama, E.; Nakamura, T.; Itadani, H.; Tanaka, K. Identification of membrane-type receptor for bile acids (M-BAR). *Biochem. Biophys. Res. Commun.* **2002**, *298*, 714–719. [[CrossRef](#)]
19. Kawamata, Y.; Fujii, R.; Hosoya, M.; Harada, M.; Yoshida, H.; Miwa, M.; Fukusumi, S.; Habata, Y.; Itoh, T.; Shintani, Y.; et al. A G protein-coupled receptor responsive to bile acids. *J. Biol. Chem.* **2003**, *278*, 9435–9440. [[CrossRef](#)]
20. Jiao, Y.; Lu, Y.; Li, X.Y. Farnesoid X receptor: A master regulator of hepatic triglyceride and glucose homeostasis. *Acta Pharmacol. Sin.* **2015**, *36*, 44–50. [[CrossRef](#)]
21. Wang, H.; Chen, J.; Hollister, K.; Sowers, L.C.; Forman, B.M. Endogenous bile acids are ligands for the nuclear receptor FXR/BAR. *Mol. Cell* **1999**, *3*, 543–553. [[CrossRef](#)] [[PubMed](#)]
22. Liu, M.; Wang, Z.; Feng, D.; Shang, Y.; Li, X.; Liu, J.; Li, C.; Yang, Z. An Insulin-Inspired Supramolecular Hydrogel for Prevention of Type 1 Diabetes. *Adv. Sci.* **2021**, *8*, 2003599. [[CrossRef](#)] [[PubMed](#)]
23. Sun, L.; Cai, J.; Gonzalez, F.J. The role of farnesoid X receptor in metabolic diseases, and gastrointestinal and liver cancer. *Nat. Rev. Gastroenterol. Hepatol.* **2021**, *18*, 335–347. [[CrossRef](#)] [[PubMed](#)]
24. Ferretti, G.; Bacchetti, T.; Negre-Salvayre, A.; Salvayre, R.; Dousset, N.; Curatola, G. Structural modifications of HDL and functional consequences. *Atherosclerosis* **2006**, *184*, 1–7. [[CrossRef](#)]
25. Van der Steeg, W.A.; Holme, I.; Boekholdt, S.M.; Larsen, M.L.; Lindahl, C.; Stroes, E.S.; Tikkanen, M.J.; Wareham, N.J.; Faergeman, O.; Olsson, A.G.; et al. High-density lipoprotein cholesterol, high-density lipoprotein particle size, and apolipoprotein A-I: Significance for cardiovascular risk: The IDEAL and EPIC-Norfolk studies. *J. Am. Coll. Cardiol.* **2008**, *51*, 634–642. [[CrossRef](#)]
26. Hageman, J.; Herrema, H.; Groen, A.K.; Kuipers, F. A role of the bile salt receptor FXR in atherosclerosis. *Arter. Arterioscler. Thromb. Vasc. Biol.* **2010**, *30*, 1519–1528. [[CrossRef](#)]
27. Pellicciari, R.; Gioiello, A.; Macchiarulo, A.; Thomas, C.; Rosatelli, E.; Natalini, B.; Sardella, R.; Pruzanski, M.; Roda, A.; Pastorini, E.; et al. Discovery of 6 $\alpha$ -ethyl-23(S)-methylcholic acid (S-EMCA, INT-777) as a potent and selective agonist for the TGR5 receptor, a novel target for diabetes. *J. Med. Chem.* **2009**, *52*, 7958–7961. [[CrossRef](#)]
28. Pellicciari, R.; Passeri, D.; De Franco, F.; Mostarda, S.; Filipponi, P.; Colliva, C.; Gadaleta, R.M.; Franco, P.; Carotti, A.; Macchiarulo, A.; et al. Discovery of 3 $\alpha$ ,7 $\alpha$ ,11 $\beta$ -Trihydroxy-6 $\alpha$ -ethyl-5 $\beta$ -cholan-24-oic Acid (TC-100), a Novel Bile Acid as Potent and Highly Selective FXR Agonist for Enterohepatic Disorders. *J. Med. Chem.* **2016**, *59*, 9201–9214. [[CrossRef](#)]
29. Nakhi, A.; McDermott, C.M.; Stoltz, K.L.; John, K.; Hawkinson, J.E.; Ambrose, E.A.; Khoruts, A.; Sadowsky, M.J.; Dosa, P.I. 7-Methylation of Chenodeoxycholic Acid Derivatives Yields a Substantial Increase in TGR5 Receptor Potency. *J. Med. Chem.* **2019**, *62*, 6824–6830. [[CrossRef](#)]
30. Hanafi, N.I.; Mohamed, A.S.; Kadir, S.H.S.A.; Othman, M.H.D. Overview of Bile Acids Signaling and Perspective on the Signal of Ursodeoxycholic Acid, the Most Hydrophilic Bile Acid, in the Heart. *Biomolecules* **2018**, *8*, 159. [[CrossRef](#)]
31. Fujiwara, R.; Chen, S.; Karin, M.; Tukey, R.H. Reduced expression of UGT1A1 in intestines of humanized UGT1 mice via inactivation of NF-kappaB leads to hyperbilirubinemia. *Gastroenterology* **2012**, *142*, 109–118.e2. [[CrossRef](#)] [[PubMed](#)]

32. Bernstein, H.; Bernstein, C.; Payne, C.M.; Dvorak, K. Bile acids as endogenous etiologic agents in gastrointestinal cancer. *World J. Gastroenterol.* **2009**, *15*, 3329–3340. [[CrossRef](#)] [[PubMed](#)]
33. Goossens, J.F.; Bailly, C. Ursodeoxycholic acid and cancer: From chemoprevention to chemotherapy. *Pharmacol. Ther.* **2019**, *203*, 107396. [[CrossRef](#)]
34. Buryova, H.; Chalupsky, K.; Zbodakova, O.; Kanchev, I.; Jirouskova, M.; Gregor, M.; Sedlacek, R. Liver protective effect of ursodeoxycholic acid includes regulation of ADAM17 activity. *BMC Gastroenterol.* **2013**, *13*, 155. [[CrossRef](#)] [[PubMed](#)]
35. Mohamed, A.S.; Hanafi, N.I.; Kadir, S.H.S.A.; Noor, J.; Hasani, N.A.H.; Ab Rahim, S.; Siran, R. Ursodeoxycholic acid protects cardiomyocytes against cobalt chloride induced hypoxia by regulating transcriptional mediator of cells stress hypoxia inducible factor 1 $\alpha$  and p53 protein. *Cell Biochem. Funct.* **2017**, *35*, 453–463. [[CrossRef](#)]
36. Amidon, G.L.; Lennernas, H.; Shah, V.P.; Crison, J.R. A theoretical basis for a biopharmaceutic drug classification: The correlation of in vitro drug product dissolution and in vivo bioavailability. *Pharm. Res.* **1995**, *12*, 413–420. [[CrossRef](#)]
37. Kowdley, K.V.; Luketic, V.; Chapman, R.; Hirschfield, G.M.; Poupon, R.; Schramm, C.; Vincent, C.; Rust, C.; Parés, A.; Mason, A.; et al. A randomized trial of obeticholic acid monotherapy in patients with primary biliary cholangitis. *Hepatology* **2018**, *67*, 1890–1902. [[CrossRef](#)]
38. Trauner, M.; Nevens, F.; Shiffman, M.L.; Drenth, J.P.H.; Bowlus, C.L.; Vargas, V.; Andreone, P.; Hirschfield, G.M.; Pencek, R.; Malecha, E.S.; et al. Long-term efficacy and safety of obeticholic acid for patients with primary biliary cholangitis: 3-year results of an international open-label extension study. *Lancet Gastroenterol. Hepatol.* **2019**, *4*, 445–453. [[CrossRef](#)]
39. Attili, A.F.; Angelico, M.; Cantafora, A.; Alvaro, D.; Capocaccia, L. Bile acid-induced liver toxicity: Relation to the hydrophobic-hydrophilic balance of bile acids. *Med. Hypotheses* **1986**, *19*, 57–69. [[CrossRef](#)]
40. Yu, D.D.; Sousa, K.M.; Mattern, D.L.; Wagner, J.; Fu, X.; Vaidehi, N.; Forman, B.M.; Huang, W. Stereoselective synthesis, biological evaluation, and modeling of novel bile acid-derived G-protein coupled bile acid receptor 1 (GP-BAR1, TGR5) agonists. *Bioorg. Med. Chem.* **2015**, *23*, 1613–1628. [[CrossRef](#)]
41. Wang, Y.; Yue, Q.; Zhao, Y.; Qiu, S.; Peng, Y.; Li, J.; Zhang, T.; Hai, L.; Guo, L.; Wu, Y. First synthesis of 22-oxa-chenodeoxycholic acid analogue. *Steroids* **2016**, *110*, 70–76. [[CrossRef](#)] [[PubMed](#)]
42. Yu, D.D.; Andrali, S.S.; Li, H.; Lin, M.; Huang, W.; Forman, B.M. Novel FXR (farnesoid X receptor) modulators: Potential therapies for cholesterol gallstone disease. *Bioorg. Med. Chem.* **2016**, *24*, 3986–3993. [[CrossRef](#)] [[PubMed](#)]
43. Gu, Y.; Zhou, H.; Gan, Y.; Zhang, J.; Chen, J.; Gan, X.; Li, H.; Zheng, W.; Meng, Z.; Ma, X.; et al. Small-molecule induction of phospho-eIF4E sumoylation and degradation via targeting its phosphorylated serine 209 residue. *Oncotarget* **2015**, *6*, 15111–15121. [[CrossRef](#)] [[PubMed](#)]
44. KA, H. Sauerstoff-übertragung durch Osmiumtetroxyd und Aktivierung von Chlorat-Lösungen. *Ber. Dtsch. Chem. Ges.* **1912**, *45*, 3329.
45. VanRheenen, V.; Kelly, R.C.; Cha, D.Y. An improved catalytic OsO<sub>4</sub> oxidation of olefins to cis-1,2-glycols using tertiary amine oxides as the oxidant. *Tetrahedron Lett.* **1976**, *17*, 1973–1976. [[CrossRef](#)]
46. Chaudhari, S.N.; Harris, D.A.; Aliakbarian, H.; Luo, J.N.; Henke, M.T.; Subramaniam, R.; Vernon, A.H.; Tavakkoli, A.; Sheu, E.G.; Devlin, A.S. Bariatric surgery reveals a gut-restricted TGR5 agonist with anti-diabetic effects. *Nat. Chem. Biol.* **2021**, *17*, 20–29. [[CrossRef](#)]
47. Hodge, R.J.; Lin, J.; Vasist Johnson, L.S.; Gould, E.P.; Bowers, G.D.; Nunez, D.J.; SB-756050 Project Team. Pharmacokinetics, and Pharmacodynamic Effects of a Selective TGR5 Agonist, SB-756050, in Type 2 Diabetes. *Clin. Pharmacol. Drug Dev.* **2013**, *2*, 213–222. [[CrossRef](#)]
48. Macchiarulo, A.; Gioiello, A.; Thomas, C.; Pols, T.W.H.; Nuti, R.; Ferrari, C.; Giacchè, N.; De Franco, F.; Pruzanski, M.; Auwerx, J.; et al. Probing the Binding Site of Bile Acids in TGR5. *ACS Med. Chem. Lett.* **2013**, *4*, 1158–1162. [[CrossRef](#)]
49. Lasalle, M.; Hoguet, V.; Hennuyer, N.; Leroux, F.; Piveteau, C.; Belloy, L.; Lestavel, S.; Vallez, E.; Dorchie, E.; Duplan, I.; et al. Topical Intestinal Aminoimidazole Agonists of G-Protein-Coupled Bile Acid Receptor 1 Promote Glucagon Like Peptide-1 Secretion and Improve Glucose Tolerance. *J. Med. Chem.* **2017**, *60*, 4185–4211. [[CrossRef](#)]
50. Duan, H.; Ning, M.; Zou, Q.; Ye, Y.; Feng, Y.; Zhang, L.; Leng, Y.; Shen, J. Discovery of Intestinal Targeted TGR5 Agonists for the Treatment of Type 2 Diabetes. *J. Med. Chem.* **2015**, *58*, 3315–3328. [[CrossRef](#)]
51. Chen, T.; Reich, N.W.; Bell, N.; Finn, P.D.; Rodriguez, D.; Kohler, J.; Kozuka, K.; He, L.; Spencer, A.G.; Charlot, D.; et al. Design of Gut-Restricted Thiazolidine Agonists of G Protein-Coupled Bile Acid Receptor 1 (GPBAR1, TGR5). *J. Med. Chem.* **2018**, *61*, 7589–7613. [[CrossRef](#)] [[PubMed](#)]
52. Ma, S.Y.; Ning, M.M.; Zou, Q.A.; Feng, Y.; Ye, Y.L.; Shen, J.H.; Leng, Y. OL3, a novel low-absorbed TGR5 agonist with reduced side effects, lowered blood glucose via dual actions on TGR5 activation and DPP-4 inhibition. *Acta Pharmacol. Sin.* **2016**, *37*, 1359–1369. [[CrossRef](#)]
53. Kundu, S.; Bansal, S.; Muthukumarasamy, K.M.; Sachidanandan, C.; Motiani, R.K.; Bajaj, A. Deciphering the role of hydrophobic and hydrophilic bile acids in angiogenesis using in vitro and in vivo model systems. *MedChemComm* **2017**, *8*, 2248–2257. [[CrossRef](#)] [[PubMed](#)]
54. Lipinski, C.A.; Lombardo, F.; Dominy, B.W.; Feeney, P.J. Experimental and computational approaches to estimate solubility and permeability in drug discovery and development settings. *Adv. Drug Deliv. Rev.* **2001**, *46*, 3–26. [[CrossRef](#)] [[PubMed](#)]

55. Yang, F.; Mao, C.; Guo, L.; Lin, J.; Ming, Q.; Xiao, P.; Wu, X.; Shen, Q.; Guo, S.; Shen, D.-D.; et al. Structural basis of GPBAR activation and bile acid recognition. *Nature* **2020**, *587*, 499–504. [[CrossRef](#)]
56. Guo, X.; Chen, Z.; Xia, Y.; Lin, W.; Li, H. Investigation of the genetic variation in ACE2 on the structural recognition by the novel coronavirus (SARS-CoV-2). *J. Transl. Med.* **2020**, *18*, 321. [[CrossRef](#)]

**Disclaimer/Publisher’s Note:** The statements, opinions and data contained in all publications are solely those of the individual author(s) and contributor(s) and not of MDPI and/or the editor(s). MDPI and/or the editor(s) disclaim responsibility for any injury to people or property resulting from any ideas, methods, instructions or products referred to in the content.